LFP Analysis of Brain Injured Anesthetized Animals Undergoing Closed-Loop Intracortical Stimulation

Alberto Averna, *Member, IEEE*, Federico Barban, *Member, IEEE*, Marta Carè, *Member, IEEE*, Maxwell D. Murphy, Riccardo Iandolo, *Member, IEEE*, Lorenzo De Michieli, *Member, IEEE*, Randolph J. Nudo, David J. Guggenmos, and Michela Chiappalone, *Member, IEEE*

***Abstract*— Activity dependent stimulation (ADS) is a closed loop stimulation technique whose neurophysiological effects have not been deeply investigated. Here we explored how Local field Potentials (LFP) are impacted by a focal ischemic lesion and, subsequently, by ADS treatment. Intracortical microelectrode arrays were implanted in the rostral forelimb area (RFA) and in the primary somatosensory area (S1) of anaesthetized rats. An ischemic injury was induced in the caudal forelimb area through microinjections of Endothelin-1. The lesion induced an acute depressive trend in LFP power in RFA (evaluated in 6 bands of interest: Delta (1–4Hz), Theta (4–8Hz), Alpha (8-11Hz), Beta (11–30Hz), LowGamma (30–55Hz) and HighGamma (55-80)) followed by a noticeable significant rebound in both areas. Applying ADS induced an overall decrease of power. The lesion impacted the connectivity in a frequency specific manner, resulting in widespread increase in connectivity in Delta both between and within areas. Two hours after the lesion, without stimulation, correlated activity between areas increased in Beta and Gamma. After stimulation, inter-area connectivity increased in Delta, Theta and Alpha, while considerably dropping within RFA in highGamma. By computing phase-amplitude coupling, we found that the lesion produced an incremental increase in the coupling between (Theta) Alpha phase and (lowGamma) highGamma amplitude within RFA, while S1 had a more generalized increase. Likewise, coupling between Theta phase and lowGamma/highGamma amplitudes increased between areas after lesion. ADS induced a similar increase, but greater in magnitude both within and between RFA and S1. These results have important implications on the emerging field of closed-loop adaptive stimulation promoting ADS as an innovative tool for the treatment of neurological disorders.**

***Index Terms*— Activity-dependent stimulation, connectivity, in vivo, local field potential, micro-electrode arrays, phase amplitude coupling, power envelope correlation.**

Manuscript received November 8, 2021; revised March 18, 2022; accepted May 3, 2022. Date of publication May 23, 2022; date of current version June 1, 2022. The work of Michela Chiappalone was supported by the Italian Ministry of Foreign Affairs and International Collaboration (MAECI), Directorate General for Country Promotion (as a high-relevance bilateral project within the Italy–USA). The work of Randolph J. Nudo was supported by the National Institutes of Health under Grant R01NS030853. The work of David J. Guggenmos was supported by the National Institutes of Health under Grant 5R03HD094608. *(Alberto Averna and Federico Barban are co-first authors.) (David J. Guggenmos and Michela Chiappalone are co-last authors.) (Corresponding author: Michela Chiappalone.)*

Alberto Averna was with the Rehab Technologies, Istituto Italiano di Tecnologia, 16163 Genoa, Italy. He is now with the Department of Neurology, and the Bern University Hospital, University of Bern, 3010 Bern, Switzerland (e-mail: alberto.averna@insel.ch).

Federico Barban, Marta Carè, and Michela Chiappalone are with the Rehab Technologies, Istituto Italiano di Tecnologia, 16163 Genoa, Italy, and also with the Department of Informatics, Bioengineering, Robotics and System Engineering (DIBRIS), University of Genoa, 16145 Genoa, Italy (e-mail: federico.barban@iit.it; marta.care@iit.it; michela.chiappalone@iit.it).

Maxwell D. Murphy was with the Department of Rehabilitation Medicine, and the Landon Center on Aging, University of Kansas Medical Center, Kansas City, KS 66160 USA. He is now with the Neuroscience Institute, Carnegie Mellon University, Pittsburgh, PA 15213 USA (e-mail: mdmurphy@andrew.cmu.edu).

Riccardo Iandolo was with the Rehab Technologies, Istituto Italiano di Tecnologia, 16163 Genoa, Italy. He is now with the Department of Neuromedicine and Movement Science, Norwegian University of Science and Technology, 7034 Trondheim, Norway (e-mail: riccardo.iandolo@ntnu.no).

Lorenzo De Michieli is with the Rehab Technologies, Istituto Italiano di Tecnologia, 16163 Genoa, Italy (e-mail: lorenzo.demichieli@iit.it).

Randolph J. Nudo and David J. Guggenmos are with the Department of Rehabilitation Medicine, and the Landon Center on Aging, University of Kansas Medical Center, Kansas City, KS 66160 USA (e-mail: rnudo@kumc.edu; dguggenmos@kumc.edu).

Digital Object Identifier 10.1109/TNSRE.2022.3177254

I. Introduction

NEUROLOGICAL disorders have a considerable impact on public health and are among the most important causes of mortality, constituting 12% of all deaths globally [2]. Stroke frequently impacts survivors' ability to function, significantly impairing activities of daily living, especially in people aged 65 and over [3]. About 87% of all strokes have an ischemic origin, a condition in which impaired cerebral blood circulation results in an inadequate influx of oxygen and nutrients to the brain tissue [3]. These lesions are highly disruptive, both through the initial loss of brain tissue (i.e., local change) and the interruption of communication between coordinated regions which leads to network-wide changes to regions directly and indirectly connected to the site of injury. Behavioral outcomes of a stroke therefore reflect both local and global changes in activity, resulting in sensorimotor or cognitive dysfunctions, often classified to as disconnection syndromes [4], [5].

Over the past two decades, results from neurophysiological studies in animal models and neuroimaging studies in human populations [6], [7] have suggested that neuroplasticity in the remaining, intact tissue underlies functional recovery after brain injury [8]. Essentially, every therapeutic approach in post-stroke rehabilitation relies on neuroplasticity. However, even if restorative treatments based on physical therapy represent the standard-of-care, they have demonstrated limited

efficacy [9]. Indeed, there is a growing body of evidence pointing at electroceutical approaches as viable additions to, if not as alternatives for, standard treatments [10]–[12].

Results in animal models [13] have demonstrated that intracortical microstimulation (i.e., ICMS) can be used successfully to assist in guiding appropriate de novo functional connections to restore lost sensorimotor integration. A specific type of ICMS, namely activity-dependent stimulation (ADS), utilizes the intrinsic neural activity recorded in one population of neurons to trigger, through electrical stimulation, the evoked activity in another population, in a closed-loop paradigm [14]. ADS can effectively promote behavioral recovery by re-establishing an artificial connection between the Rostral Forelimb Area (i.e., RFA, the premotor cortex analogue in rats) and the Primary Somatosensory Cortex (S1) following primary motor cortical (M1) injury [13].

We recently reported that closed-loop stimulation of S1 through the ADS paradigm was able to alter the evoked response of RFA over random stimulation by modulating cortico-cortical connectivity in both anesthetized [15] and behaving [1] healthy rats. Because ADS is intended to be a therapy after brain injury, it is necessary to investigate the impact closed-loop stimulation has immediately following a disruption to the sensorimotor networks. Further, the impact of ADS may be variable depending on if it is applied during acute, sub-acute, or chronic phases of the injury.

In this study we performed acute experiments in anesthetized rats undergoing a focal lesion in the primary motor area. We recorded the electrophysiological activity of both RFA and S1, in order to evaluate *i*) the local and global impact of the focal lesion in spared premotor and somatosensory areas and *ii)* the ability of acute ADS to significantly alter this activity in the acute stage of injury. Using Local Field Potentials (LFPs), we first investigated how the power in the different bands was influenced by either the lesion or the stimulation. We then computed the phase-amplitude coupling (PAC), which is a measure that quantifies the level of synchronization between the phase of the lower frequency oscillation and the amplitude of the higher frequency oscillation. While oscillatory power is largely an indicator of integrated neuronal synchronization from a localized area [16], PAC likely reflects local or large-scale inter-network communication subserved through cross-frequency interactions [17]. We finally computed the functional connectivity according to methods devised for human studies [18]. We found that the lesion caused a noticeable but non significant drop in LFP power, especially in RFA and an increment in inter areal functional connectivity at low frequencies. Post lesion, ADS strongly modulated the LFP power and the inter-area connectivity in a frequency-specific way.

Overall, our results provide important insights into the local and global impact of a focal lesion and suggests the utility of ADS as a powerful tool to manipulate post-lesion connectivity in the acute phase of injury.

II. Materials and Methods

A. Animals

All experiments were approved by both the University of Kansas Medical Center Institutional Animal Care and Use Committee (USA: protocol 2017-2384 approved on 2/17/17) and by the Italian Ministry of Health and Animal Care (Italy: authorization ID 861/2015 PR). 12 adult male Long-Evans rats were used in total (weight: 350-400g, age: 4-5 months; Charles River Laboratories, Wilmington, MA, USA) in this study.

B. Surgical Procedures

Anaesthesia was induced by exposing the rats to gaseous isoflurane within a sealed chamber and subsequently injecting ketamine (80-100mg/kg IP) and xylazine (5-10 mg/kg IM). To maintain the anesthetized state, ketamine was administered repeatedly (10-100mg/kg/h IM) whenever a positive pinch or ocular reflex was detected. Rat temperature and vital signs were monitored continuously throughout the procedure. After securing the rat in a stereotaxic frame, ophthalmic ointment and lidocaine cream was applied and the skull was exposed through a midline scalp incision. A laminectomy was performed at the Cisterna Magna to drain the cerebrospinal fluid and prevent excessive brain swelling. Six 0.65mm holes were drilled into the skull over the dominant hemisphere's caudal forelimb area (CFA, the primary motor cortex (M1) analogue in rats) at +0.5, +2.5; +1.5, +2.5; +2.5, +2.5; +0.5, +3.5; +1.5, +3.5; +2.5, +3.5 (AP, ML) from bregma. A round craniectomy (3mm diameter) was performed over the Rostral Forelimb Area (RFA) and the Primary Somatosensory Cortex (S1), based on stereotaxic coordinates (+3.5,+2.5; −1.75,+4.25 AP,ML, respectively [19]). After removal of the dura over RFA and S1, a 4 shank 16 contact site electrode (A4 × 4.5mm-100-125-703-A16, NeuroNexus, 1-1.5 MΩ) was inserted at a depth of 1700 μm. An ischemic lesion was induced by injecting Endothelin-1 (ET-1, 0.3μg dissolved in 1μl saline solution, 3nl/sec, Bachem Americas, USA), a potent vasoconstrictor, in each of the 6 burr holes over CFA [20], [21]. A schematic of the implanted rat with the involved cortical areas is reported in Fig. 1A.

C. Experimental Protocol

Electrophysiological recordings were performed at 30kHz and 16bit of depth (RHS 2000, Intan technologies LLC). The animals were randomly assigned to two groups: a stimulation group (N=7 for ADS, for Activity Dependent Stimulation) and a control group (N=5 for CTR) which did not receive any kind of stimulation. Two animals from the ADS group were discarded during analysis due to a very poor signal quality, bringing the total for ADS to N=5.

ADS was delivered through a single channel on the S1 probe and consisted of single pulse 60μA, 200μs, biphasic, cathodal leading square waves. Each stimulation pulse was triggered by the detection of a spike (identified by manually set threshold detector based on visual inspection) on a user defined channel on the RFA probe as described in [15] (Fig 1B). The latency between the detection and the stimulation was set to 10ms, followed by a 18ms "blanking" period where no other pulse could be delivered. This results in a multi-peaked distribution with a 6.99Hz (1.2Hz to 30.4Hz, 5th to 95th percentile) median stimulation frequency.

While the animal preparation was identical, there were methodological differences between ADS and CTR due to differences in stereological equipment at the two testing

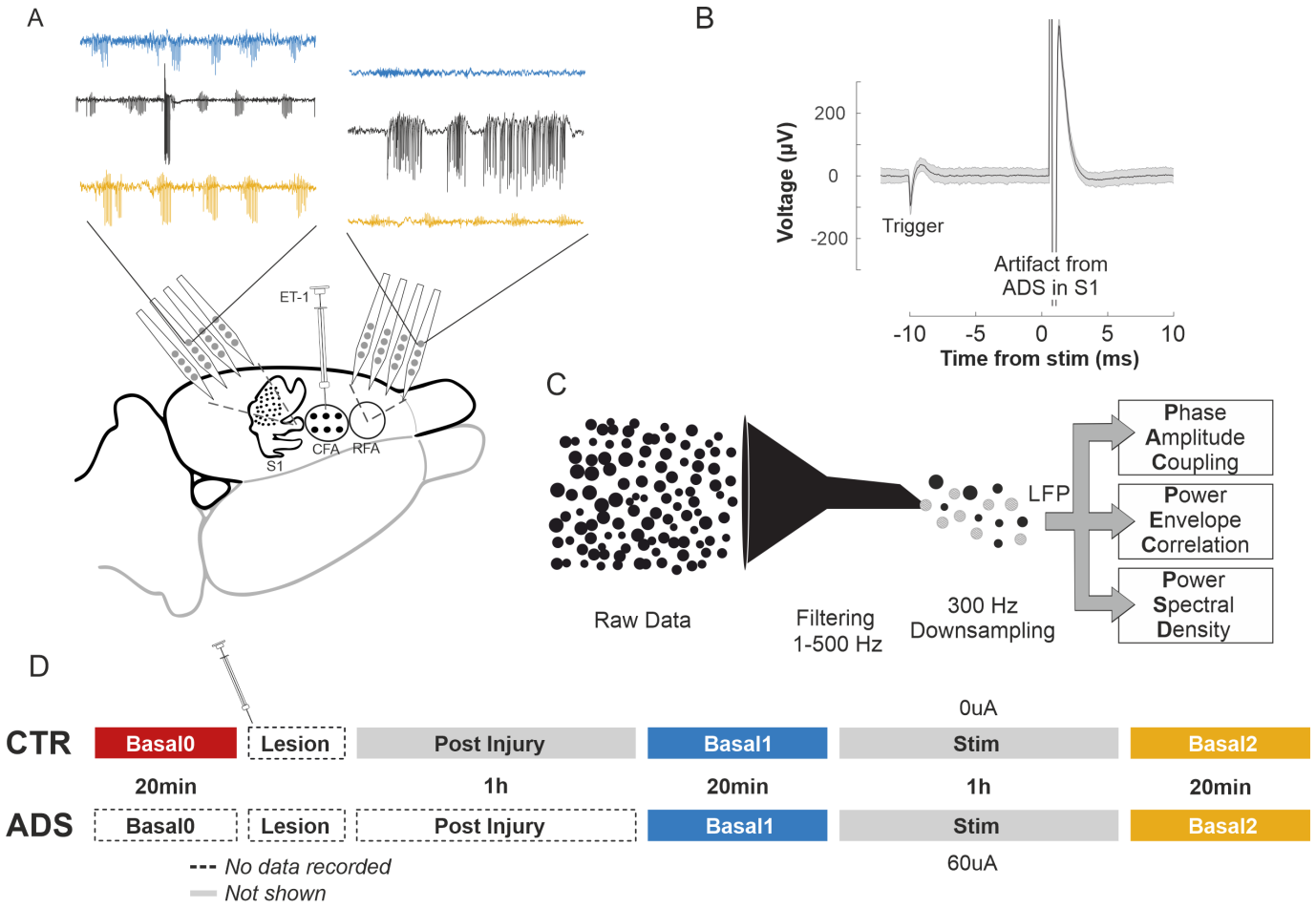

Fig. 1. Experimental protocol and data analysis procedure in injured anesthetized animals. A) The experimental scheme of an implanted rat is presented. Two multisite electrodes were implanted in the left hemisphere, i.e., in the Rostral Forelimb Area – RFA for recording, and in the Primary Somatosensory area - S1 for recording and stimulation. The lesion site was located in the Caudal Forelimb Area, CFA. On the top, raw signals in the recording sites (i.e. RFA and S1) from a representative ADS animal (from top to bottom: Basal1, Stim, Basal2 – see D for the explanation). B) Sample trace of recordings in RFA showing the mechanism of ADS. Both the stimulus artifacts from ADS delivered to S1 and activity of the trigger unit are visible. The average of 100 traces is shown, depicted as mean ± STD. Adapted from [1]. C) Block diagram of data analysis. Briefly, raw data was band-pass filtered in the range 1-500 Hz and downsampled at 300Hz to obtain Local Field Potentials (LFPs). LFPs were then analyzed in terms of Power Spectral Density, Phase Amplitude Coupling and Power Envelope Correlation. D) Experimental timeline of the two experimental groups, i.e. CTR (Control) and ADS. Control experiments (top sketch) were characterized by five phases of spontaneous activity recording (Basal 0, Basal1 and Basal2 of 20 min each, Post Injury and Stim of 60 min each) and one phase of lesion induction, where no recording was performed. In this group, for the Stim phase, the stimulation current was set to 0A for the entire recording time of 60 min. The ADS experiments (bottom sketch) were characterized by three phases, the middle one consisting of 60 minutes of stimulation (Stim) where current was delivered in the form of biphasic squared pulses at 60 uA, while the other two being characterized by 20 minutes of spontaneous activity recording, during which no stimulation was applied (i.e., Basal1 and Basal2). The colors of the Basal phases correspond to the colored profiles for the same phases in the PSD analysis (cf. Fig. 2).

locations. Initial ADS experiments at IIT required setting the electrodes after ischemic injury and remained consistent between locations. All CTR recordings were done at KUMC and allowed electrodes to be set prior to induction of the ischemic lesion. For both CTR and ADS, there was a common 100 minute period of recording initiated one hour after the last ET-1 injection that consisted of a 20 minute pre-stimulation (Basal1) period, a 60 minute stimulation period (Stim) and a 20 minute post-stimulation period (Basal2). For CTR experiments, the current delivered during the Stim phase was equal to 0μA. In the CTR group, we recorded an additional 20 minute period prior to lesion induction (Basal0) and in the 60 minutes immediately after lesion completion (Post Injury). The full protocol is summarized in Fig. 1D.

D. Data Analysis

Using a custom Matlab pipeline (Fig. 1C), recorded data was first filtered to prevent aliasing and then downsampled to 300Hz to extract the LFPs. LFPs were not re-referenced offline [22], as the subtraction of a new reference would have potentially changed both the spectral properties of the signals and coherence between channels which were both investigated in this study. Following extraction, power and connectivity analysis were performed.

1) Power Spectral Density (PSD): The power spectral density was estimated using the Welch method [Windows = 1s, overlap = 50%; DFT (Discrete Fourier Transform) points = 131073; df (frequency resolution) = 0.0023Hz;], according to [23]. The PSD was later normalized over the standard

deviation of the PSD computed on the raw signal between 200 and 300 Hz [24]. For the PSD analysis, the signal was divided in 6 bands of interest: Delta (1–4Hz), Theta (4–8Hz), Alpha (8-11Hz), Beta (11–30Hz), Low-Gamma (30–55Hz) and High-Gamma (55-80).

2) Phase Amplitude Coupling (PAC): We exploited a cross-frequency measure to analyze phase-to-amplitude modulation in our dataset through the Matlab based toolbox [25]. Phase-to-amplitude comodulograms were constructed by applying the modulation index (MI) measure [26] to multiple frequency band pairs (1 Hz bin) made up of "phase frequency" and (5 Hz bin) "amplitude frequency" bands. MI was calculated both locally (i.e., RFA-RFA and S1-S1) and by switching phase and amplitude from the two locations (i.e. RFA-S1 and S1-RFA), denoted respectively local-PAC (l-PAC) and switched-PAC (swPAC). To assess the statistical significance of the MI values, this was compared against a distribution of 50 shuffled time series obtained by cutting the data into 1s sections. The boundaries of the sections are placed at random locations throughout the signal and then randomly rearranged to create the final shuffled signal. This procedure removes the temporal relationship between amplitude values whilst retaining the mean, variance and power spectrum of the original signal [25]. The statistical significance of each PAC value was determined by testing against the distribution of shuffled PAC: MI values lying in the top 5% of this distribution (after Bonferroni correction) were deemed significant. A Z-score statistic for significant MI was then obtained by comparing the original values against the means and the standard deviation of the shuffled MI.

3) Power Envelope Correlation: The power envelope correlation was used as a measure of connectivity as shown in [18]. Briefly, from each signal a spectrogram with a 1Hz resolution is derived. A Pearson correlation is then computed between the squared modulus of this complex signal for each corresponding frequency bin at different spatial locations. An *atanh* transformation is used to enhance Gaussianity. To assess the statistical significance of the correlations, we compared them against a null distribution obtained by the correlations between surrogates' signals.

Fifty shuffled time series were obtained by dividing the data into 1s sections, according to [25]. The sections were randomly rearranged throughout the duration of signal to create the final shuffled data. This procedure removed the temporal relationship between amplitude values while retaining mean, variance and power spectrum of the original signal. A Z-score was obtained by comparing the real values against the surrogates: correlations were considered significant for a Z-score greater than 4.15 (standard 5% significance Bonferroni corrected for multiple comparisons, specifically 6 bands$*32*31/2$ correlations multiple comparisons). Changes in connectivity patterns were evaluated by calculating the ratio between post and pre connectivity after both lesion (Basal1/Basal0) and stimulation (Basal2/Basal1). We considered a change in connectivity for variations above or below 20% [27]–[29].

4) Statistics: Changes in LFP power were modeled and compared using a linear mixed effects model (LMM, implemented using R's lmer function). The model was designed to properly account for the dependence between different channels in the same animal by including random intercepts both at the animal and at the channels within animal level. We also decided to account for animals' individual response to the ischemic lesion by including random slopes on time at those levels [30]–[32].

Results describing PAC and correlation-based connectivity were tested for statistical significance using a surrogate analysis. Surrogate signals were derived using a shuffling procedure and used to build a null distribution. Each correlation and MI value was then tested against its respective null model correcting for multiple comparisons using Bonferroni. Prior to Bonferroni correction, the significance level was always set to p=0.05.

III. Results

A. The Lesion Induces a Decreasing Trend in LFP Power

We compared the power of the LFP signal recorded in RFA and S1 in the CTR group before and after the ischemic lesion.

Immediately following the lesion (i.e., post-Injury phase, not shown), we observed a noticeable, despite not significant, increase in LFP power in S1 with respect to Basal0, especially in Delta where power increased more than trifold ($p > 0.15$ LMM, data not shown). In RFA no major changes were observed (not shown).

The acute effect of the lesion (i.e., Basal1 phase, one hour post-lesion), brought a noticeable albeit non significant decrease of power throughout the spectrum in RFA. This effect was mostly visible in Theta, where mean power was reduced by 4.5 times, and Alpha, where it decreased by 2.8 times (Fig. 2 A1 and A2). This effect was more modest in S1, where the biggest effect was found in the same bands but only of 2 and 1.3 times respectively (Fig. 2 B1 and B2).

B. ADS Modulates LFP Power

We computed the power of the LFP signal recorded before (Basal1) and after (Basal2) the stimulation phase and compared it across the same period in unstimulated rats. In the CTR group, we observed a generalized increase in LFP power in both monitored areas. All bands in both areas reached significance except Theta in RFA, while S1 showed bigger and more consistent effect sizes (LMM Basal1/Basal2 for S1 ranging from 0.23 in Theta to 0.12 in Gamma, all bands $p < 5 \cdot 10^{-5}$, Fig 3B). In RFA the increase in power was moderate but still noticeable (LMM Basal1/Basal2 ranging from 0.6 in Theta to 0.13 in HGamma, Alpha p=0.012, Beta $p < 5 \cdot 10^{-3}$, Delta and Gammas $p < 5 \cdot 10^{-5}$ Fig 3A). Conversely, after ADS, we observed a widespread decreasing trend in LFP power in both regions and in all bands except for Beta. We found a significant decrease of power in the High Gamma band of RFA (LMM Basal1/Basal2 = 2.8, RFA: High Gamma p=0.002, Fig. 3C) as well as a significant decrease of Delta, Theta and HighGamma bands in S1 (LMM Basal1/Basal2 = 2.7, 2.5 and 3.8 respectively, S1: Delta p=0.003; High Gamma p=0.007, Theta $p = 5.4 \cdot 10^{-5}$ Fig. 3D). A comparison between the two groups revealed a clear effect of the stimulation

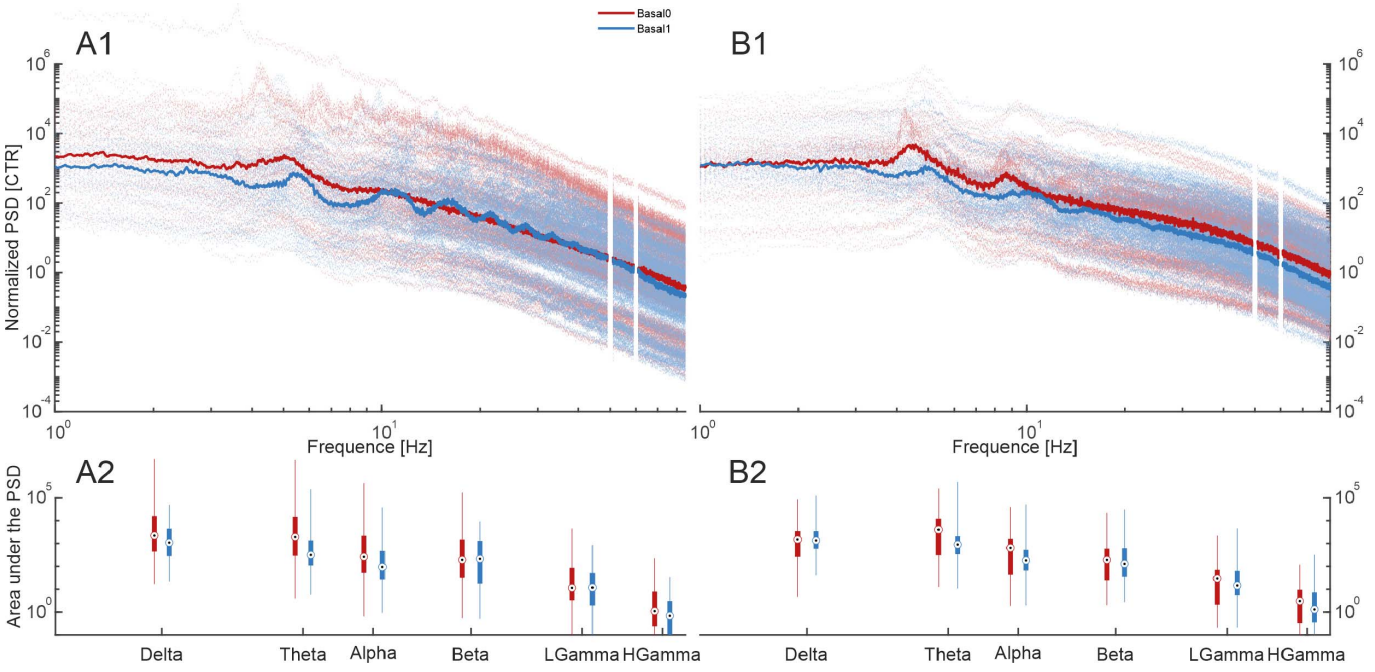

Fig. 2. Power Spectral Density (PSD) in CTR experiments, before and after the lesion. A comparison of the normalized PSDs between before (i.e. Basal0, red) and after lesion (i.e. Basal1, blue) is presented on the left for RFA and on the right for S1. On the top, in A1) and B1), the thin dotted lines represent the PSD profile of all the channels from each MEA (16 in RFA and 16 in S1) in all the animals. The thick solid line is the median value. The white blank periods are the effect of the notch filter used to blank the power line at 50Hz (Italian experiments) and 60Hz (USA experiments). On the bottom, in A2) and B2), the area under each PSD curve over the canonical LFP bands (i.e. Delta, Theta, Alpha, Beta, Low Gamma and High Gamma, cf. Data Analysis – Power Spectral Density) is presented. Data is summarized in boxplots, where the black dot inside the central target indicates the median value and the box denotes the 25th and 75th percentile, respectively. Whiskers extend to the most extreme data points. No contrasts reached significance.

in both RFA (Fig 4A) and S1 (Fig 4B) across all frequencies (LMM Basal2/Basal1 CTR/ADS, RFA: Delta $p<.0001$; Theta $p=0.003$; Alpha $p<.001$; Low Gamma $p<.0001$; High Gamma $p<.0001$; and S1: Delta $p<.0001$; Theta $p<.0001$; Alpha $p<.0001$; Beta $p<.0001$; Low Gamma $p<.0001$; High Gamma $p<.0001$).

C. Lesion and ADS Increase Both Local and Switched PAC

Before lesion, both RFA and S1 revealed Theta/Alpha-low Gamma (phases ~5-10Hz, amplitude ~30-55Hz coupling) and Theta/Alpha- high Gamma (phases ~5-10Hz, amplitude ~60-100Hz coupling) lPAC, despite S1 showed higher intensity values (Fig. 5A1). SwPAC between RFA and S1 (i.e., phases of RFA and amplitudes of S1) presented a coupling between both Theta-lowGamma and Theta/Alpha-highGamma, while S1-RFA swPAC showed only a Theta-lowGamma coupling (Fig. 5A1). After stroke an incremental increase (from Basal0 to Basal1) of Theta/Alpha-low Gamma/high Gamma lPAC was found for RFA, while S1 had a more generalized increased of lPAC which involved all the frequencies with a Theta-high Gamma lPAC peak (Fig. 5A1, A2). RFA-S1 swPAC also showed an increase of both Theta-lowGamma/highGamma coupling after stroke, with the induction of a Beta-highGamma peak in Basal2, while S1-RFA swPAC only showed incremental increase of Theta-lowGamma/highGamma coupling (Fig. 5A1, A2). Before stimulation, the ADS group presented a general low lPAC and swPAC for all RFA showed an increase of Theta/Alpha-lowGamma/highGamma coupling, while S1 presented a more spread increase of lPAC (Fig. 5B1, B2). Both RFA-S1 and S1-RFA couplings showed a localized increase in Theta/Alpha - Low/HighGamma swPAC after ADS stimulation (Fig. 5B1, B2). Relative increase (ΔZscored MI) between Basal2 and Basal1 of both lPAC and swPAC induced by ADS was higher than increase of Control group (Fig. 5C).

D. Lesion Strongly Manipulates the Correlation Structure Between S1 and RFA

We compared the number of functional connections within each considered area (i.e., RFA and S1) and between them (RFA vs S1) and we investigated how they varied during the experiment. We observed that the ischemic injury had a major influence on the connections in the Delta band, particularly on the inter-area connections (i.e., from RFA to S1) but also on the connection intra area (i.e., from RFA to RFA and from S1 to S1).

Indeed, we observed a net increase of the correlation in this frequency band, with more than 70% of the inter-area connections increasing their value. The intra-area connections stayed less than 60% for both S1 and RFA. This trend is reported in Fig. 6A and quantified in Fig. 7A. Specifically, Fig. 6A shows a distribution of the pre-post lesion correlation ratio across frequency bands and monitored cortical areas while Fig. 7A summarizes the fraction of increased and decreased connections.

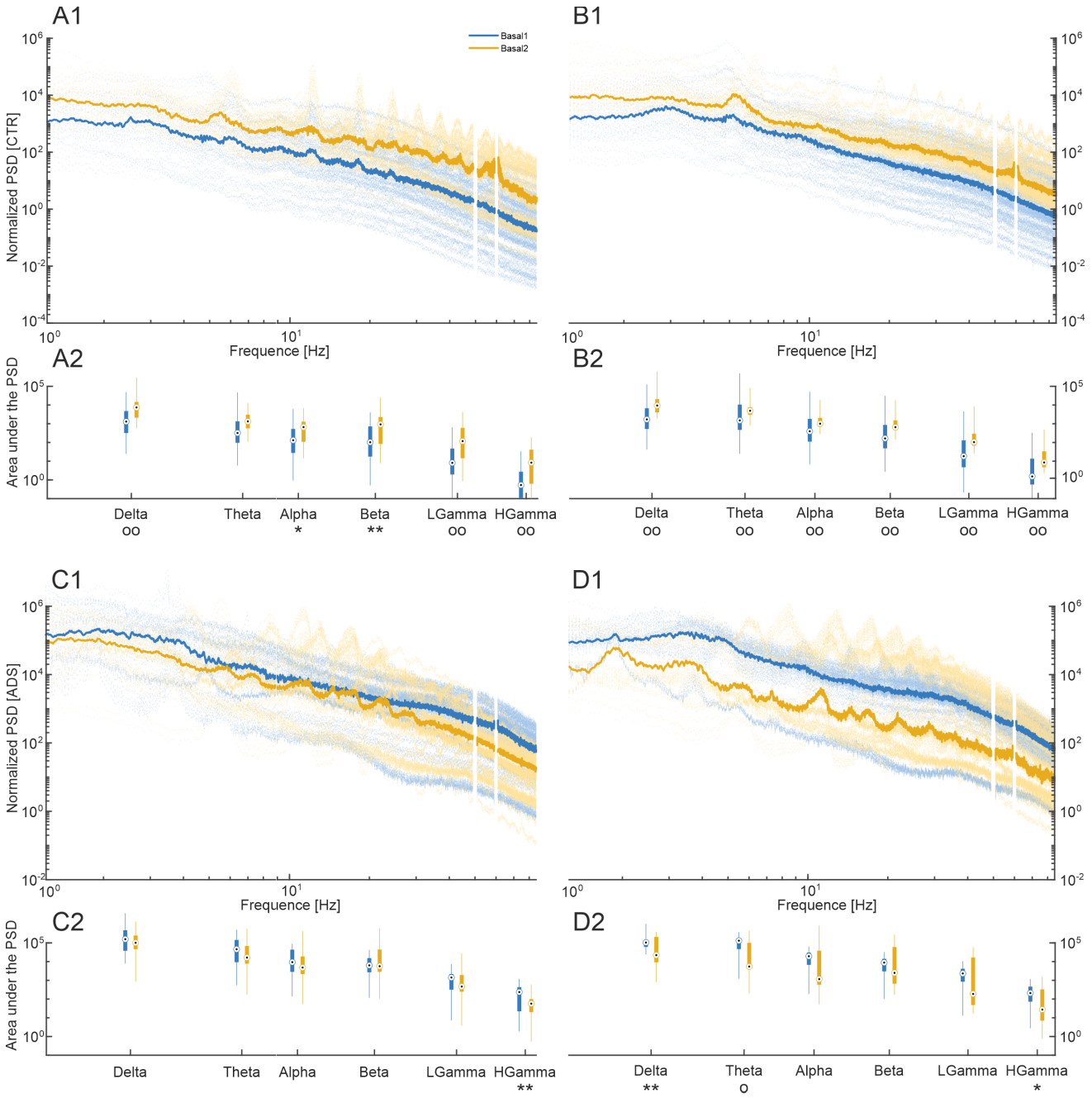

Fig. 3. Power Spectral Density (PSD) before and after stimulation. A comparison between normalized PSDs pre (i.e. Basal1, blue) and post stimulation (i.e. Basal2, yellow) is presented on the left for RFA and on the right for S1. On the top, A and B, depict the Control group, where no stimulation was delivered. A1, B1) The thin dotted lines show the PSD profile of all the channels of each MEA (16 in RFA and 16 in S1) for the entire experimental group. The thick solid line is the median value. The white lines are the effect of the notch filter used to blank the power line at 50Hz (Italian experiments) and 60Hz (USA experiments). A2, B2) The area under each PSD curve over the canonical LFP bands (cf. Data Analysis – Power Spectral Density). Data is summarized in boxplot, where the central target indicates the median value and box denotes the 25th and 75th percentile, respectively. Whiskers extend to the most extreme data points. On the bottom, C and D, show data for the ADS. As described above for the Control groups in C1, D1) each thin dotted line represents the PSD profile of all the channels of each MEA (16 in RFA and 16 in S1) for the entire experimental group. The thick solid line is the median value. C2, D2) The area under each PSD curve over the canonical LFP bands, i.e. delta, theta, alpha, beta, low gamma and high gamma (cf. Data Analysis – Power Spectral Density). Data is summarized in boxplot, where the central target indicates the median value and the box denotes the 25th and 75th percentile, respectively. Whiskers extend to the most extreme data points. $*p<5{\cdot}10^{-2}$, $**p<5{\cdot}10^{-3}$, $^{O}p<5{\cdot}10^{-4}$, $^{OO}p<5{\cdot}10^{-5}$, Linear Mixed Model (LMM).

E. ADS Modulates the Correlation Between S1 and RFA

By analyzing the number of functional connections and how they vary after the simulation (Fig. 6C), we observed an increase in the inter-area correlation strength prevalently in the Delta, Theta and Alpha bands, with a minor effect also in Beta. Intra RFA correlation mostly did not change, except for a substantial decrease in the high Gamma and a slight decrease in Delta. A small increase in Beta was also observed.

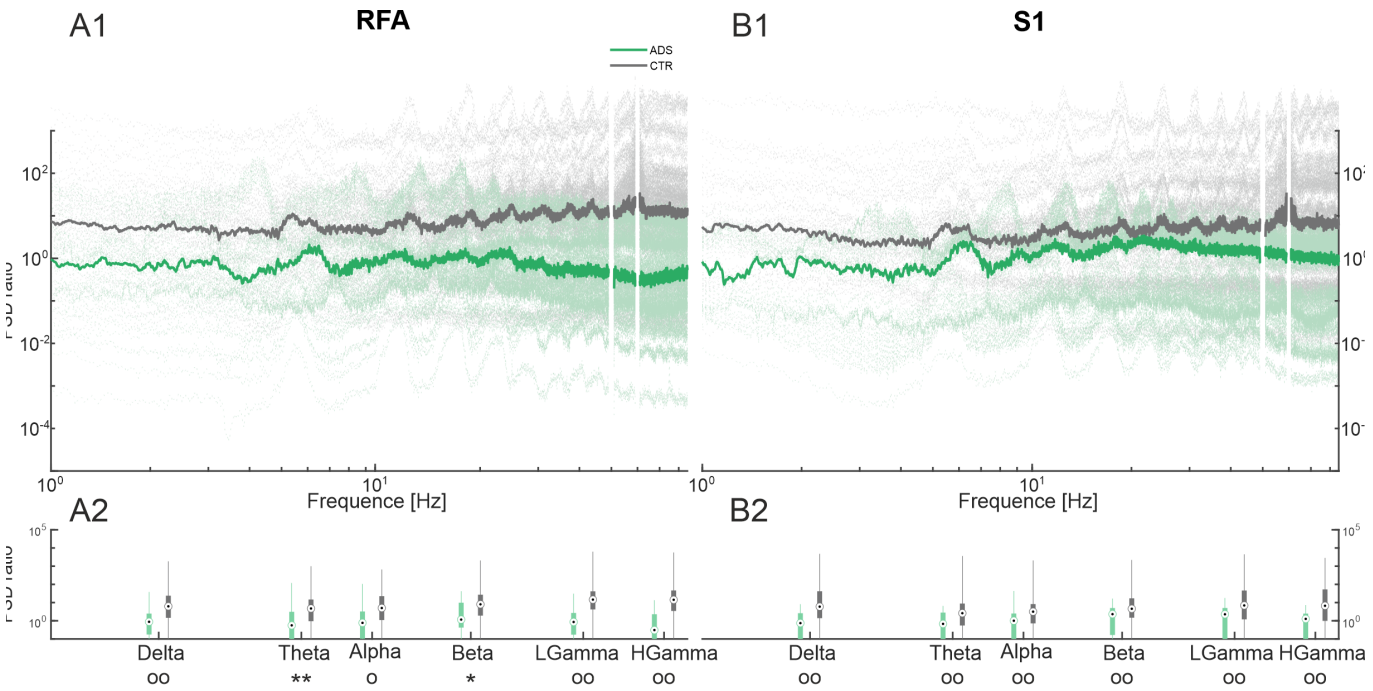

Fig. 4. Basal2/Basal1 ratio of Power Spectral Density (PSD). A comparison between CTR (grey) and ADS (green) is presented on the left for RFA and on the right for S1. On the top, in A1) and B1), the thin dotted lines represent the PSD-ratio of all the channels from each MEA (16 in RFA and 16 in S1) in all the animals. The thick solid line is the median value. The white blank periods are the effect of the notch filter used to blank the power line at 50Hz (Italian experiments) and 60Hz (USA experiments). On the bottom, in A2) and B2), the area under each PSD-ratio curve over the canonical LFP bands (cf. Data Analysis – Power spectral density) is presented. Data is summarized in boxplots, where the black dot inside the central target indicates the median value and the box denotes the 25th and 75th percentile, respectively. Whiskers extend to the most extreme data points.

In S1 we saw a broad increase in the correlation values (Delta, Theta, Alpha and Beta) with the High Gamma being mostly unaffected (Fig 7C).

The CTR group showed a tendency in the opposite direction increasing inter areal correlation values in beta and the gammas (80% and 60% respectively) while mostly leaving unaffected other frequencies except for a decrease in correlation strength in the delta band. S1 showed a small increase in Beta and Gammas while RFA only slightly increased its strength in HGamma (Fig 6B and Fig. 7B).

IV. Discussion

The purpose of this study was two-fold, 1) to investigate the early, immediate effects of an injury to M1 on the relative activity within and between the ipsilesional premotor and somatosensory areas in the rat and 2) to determine whether ADS would alter this activity in the acute phase after injury. M1 typically acts as an integrator during normal behavior, receiving motor planning information from RFA and cutaneous and proprioceptive information from S1 while having reciprocal connections to these areas.

Following ischemic injury to M1, low frequency oscillations, especially in the range of 0.5-4Hz have been implicated in the recovery process. In days 1-4 days post-lesion, spontaneous increases of power in this band have been observed and are critical for novel axonal sprouting to occur [33]. In both rodents and non-human primates, task-related power in this same band drops starting at least by day 5 post-lesion [34], [35]. The recovery of this activity seems to track with behavioral recovery, even in human stroke populations [36]. It is increasingly clear that there are mechanisms underlying these shifts that seem to be highly coupled to functional outcomes. If this activity can be induced, especially in physiologically relevant ways, it would likely lead to improved, novel therapies.

An ischemic injury to M1 leads to an immediate cascade of altered activity patterns throughout the entire sensorimotor system, including a rapid increase in glutamatergic release within the ischemic core and into the penumbra. This results in increased activity and potentially an excitotoxic response that leads to further cell death which is thought to occur rapidly after the ischemic event. While our electrodes were not directly in the penumbra, we expected a rapid, global increase in power between Basasl0 and Basal1. However, we did not observe significant change in power between Basal0 and Basal1 but instead saw this global significant increase in power between Basal1 and Basal 2 in the non-stimulated group, suggesting the slow emergence of some firing homeostatic mechanisms following the loss of M1 inputs and outputs propagating through the network that take some time to manifest as alterations in activity in these spared, adjacent regions. Further investigation in lesioned rats will be necessary to determine when this activity stabilizes and shifts to primarily changes in the Delta bands.

Apart from the oscillatory power, we also assessed the PAC between different frequencies. In sensorimotor research,

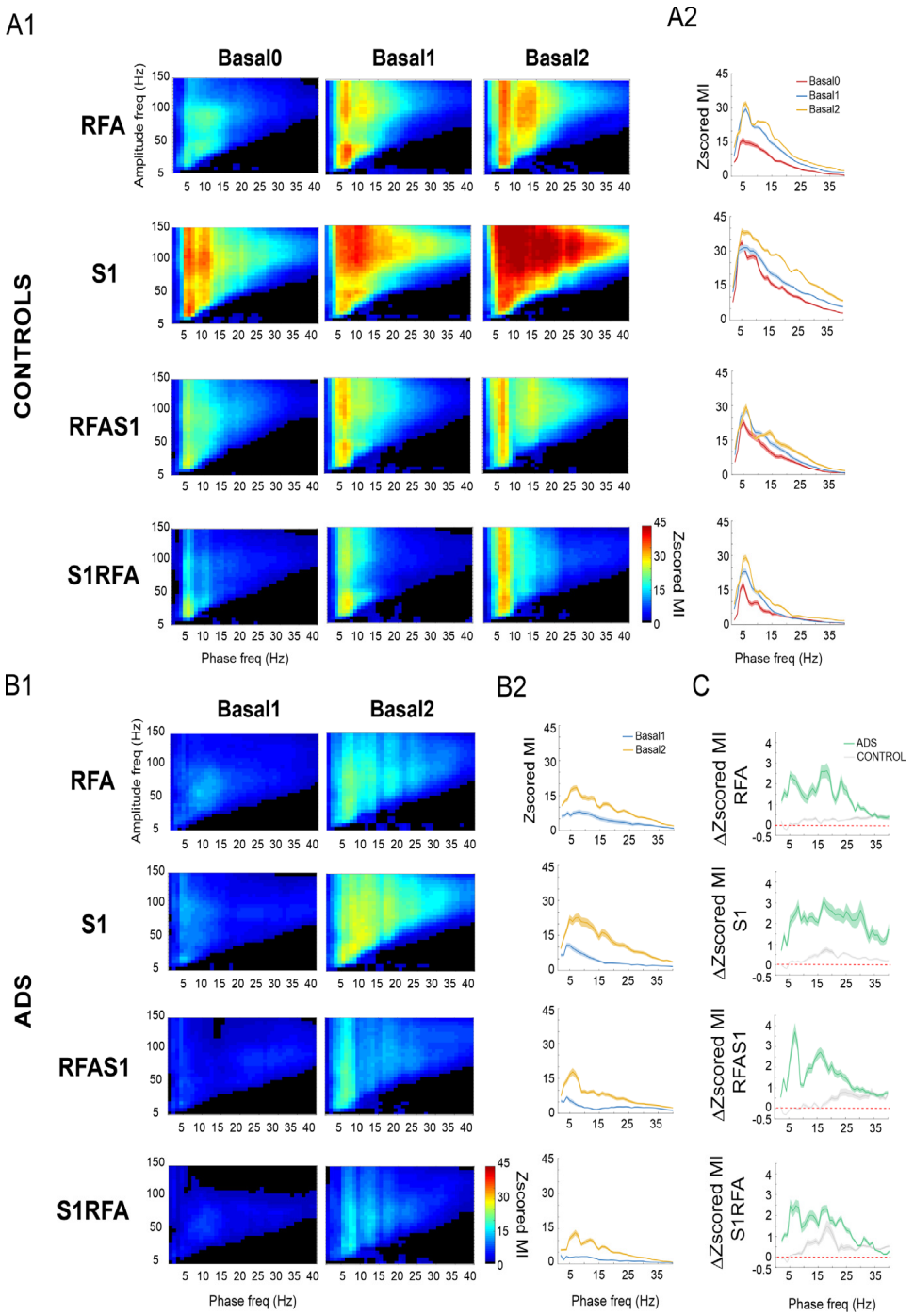

Fig. 5. Detection of PAC in local field potentials recorded simultaneously from rat RFA and S1. A1) Averaged Zscored MI analyses of continuous LFP calculated before (Basal0) and after stroke (i.e. Basal1 and Basal2) in the Control group, within (IPAC) RFA (first row, RFA) and S1 (second row, S1), and by combining (swPAC) phases of RFA with amplitudes of S1 (third row, RFAS1) and phases of S1 with amplitudes of RFA (fourth row, S1RFA). A2) Significant Zscored MI (mean +/-s.e) between averaged amplitude and phase frequency range 1-40Hz calculated before (Basal0, red) and after stroke (i.e. Basal1, blue and Basal2, yellow) within RFA (first row, RFA) and S1 (second row, S1), and between RFA and S1 (third row, RFAS1 and fourth row, S1RFA). Note incremental increase of both IPAC and swPAC induced by stroke. B1) Averaged Zscored MI analyses of continuous LFP calculated before (Basal1) and after stimulation (Basal2) in the ADS group, within RFA (first row, RFA) and S1 (second row, S1), and between RFA and S1 (third row, RFAS1 and fourth row, S1RFA). B2) Significant Zscored MI (mean +/-s.e) between averaged amplitude and phase frequency range 1-40Hz calculated before (Basal1, blue) and after stimulation (Basal2, yellow) within RFA (first row, RFA) and S1 (second row, S1), and between RFA and S1 (third row, RFAS1 and fourth row, S1RFA). Note increase of both IPAC and swPAC induced by stimulation. C) Relative variation (ΔZscored MI, Basal2-Basal1/Basal1) of significant Zscored MI between averaged amplitude and phase frequency range 1-40Hz calculated for both Control (grey line) and ADS (green line) groups within RFA (first row, RFA) and S1 (second row, S1), and between RFA and S1 (third row, RFAS1 and fourth row, S1RFA). Increase of both IPAC and swPAC was greater for ADS group.

PAC is typically used to assess relationships between cortical regions during behavioral tasks to determine how communication impacts task performance. Here, we used PAC as an investigative tool to determine if there were demonstrable shifts in the interaction between amplitude and phases of LFPs induced by ischemic injury. We observed an incremental

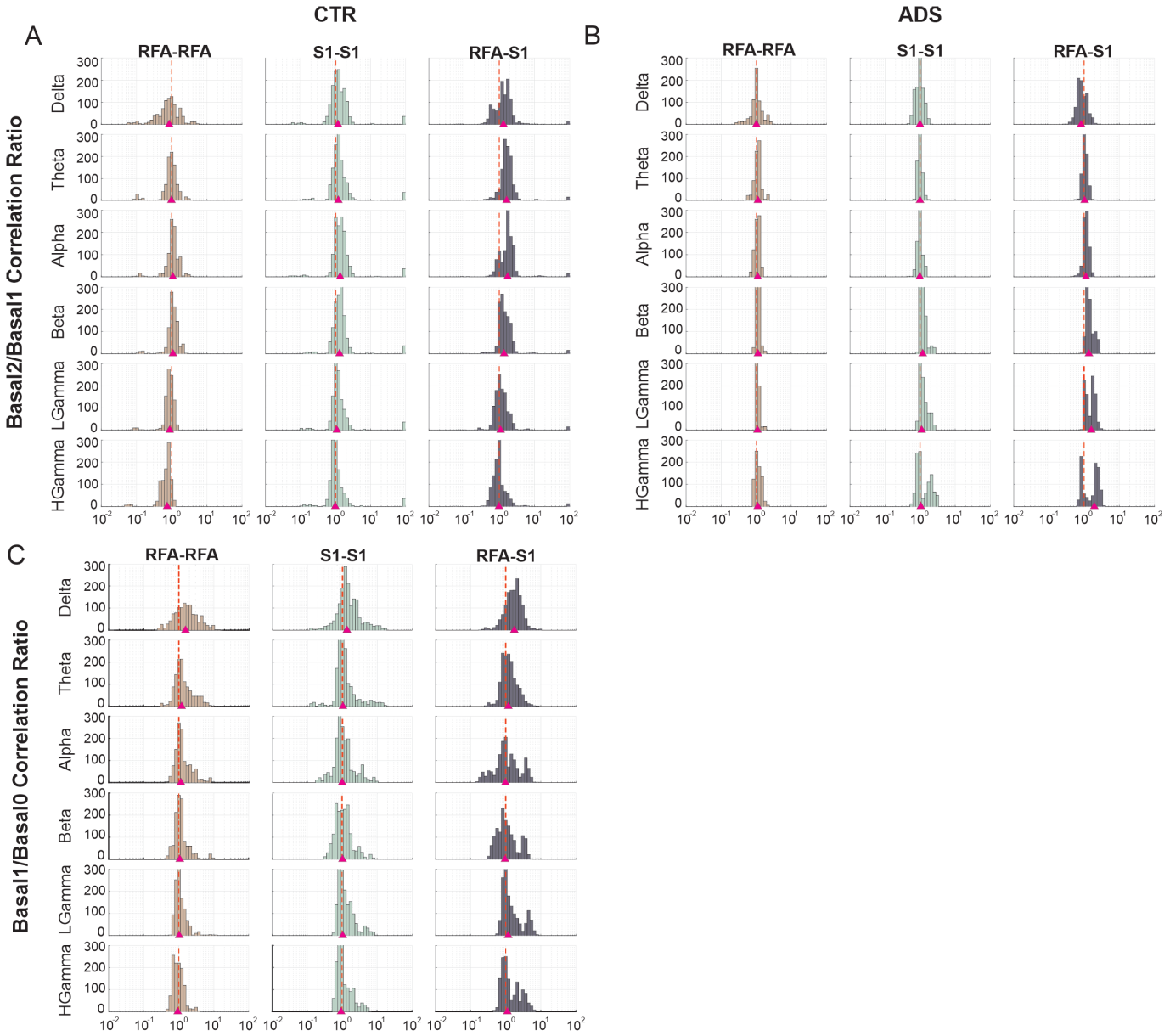

Fig. 6. Changes in connectivity patterns following stimulation and lesion. Histograms of the ratio of connectivity values before and after no stimulation, ADS and lesion (A, B and C respectively) are presented. The data is organized by frequency bands (rows) and location (columns). All channels for all animals are pooled and shown together. The x axis is logarithmic. The red dotted line indicates identity while the purple triangle shows the median of the distribution. A) Natural evolution of the network, i.e., no stimulation. A clear decrease in correlation strength between the two areas (RFA-S1) is visible in Delta. Theta and Alpha show no particular changes, with very narrow symmetrical distribution centered around 1. An increase is present in Beta, with a small increase in S1 and a substantial one in the RFA-S1 connections. A clear effect is present in the Gammas, where the correlation strength mildly increases in S1 while substantially increasing between the two areas (RFA-S1), showing again the bimodality that was also present in A. B) ADS stimulation effects. Stimulation effects almost every frequency band and in complementary manner wrt B. In Delta we see a decrease in RFA, a very slight increase in S1 and an increase in RFA-S1. Theta shows an increase in connectivity strength: mild in S1 and substantial in RFA-S1. Similar effects can be observed in Alpha and Beta. LGamma shows a decrease in RFA connectivity and only a small increase in RFA-S1. HGamma show changes only in RFA where a substantial decrease in connectivity is recorded. C) Effects of lesion. A clear shift is visible in Delta where a net increase in the correlation strength is present, especially between the two regions (RFA-S1). Globally, distributions show a tendency being skewed towards an increased connectivity, even showing bimodal shapes like in Beta and in the Gammas.

increase of Theta-Gamma PAC both within and between RFA and S1. As reported in several studies, Theta–Gamma PAC is usually involved in memory processes and long-range cortico-cortical communication [37]–[40]. Despite this, the presence and the functional role of PAC modulation in the context of ischemic lesion is still unknown. In other frameworks, such as for Parkinson's, the presence of exaggerated PAC values, albeit occurring at different frequencies and mainly in subcortical structures [41], [42], has been demonstrated to correlate with the severity of motor impairment [43]–[45]. Our results indicate that disruption to M1 emphasizes Theta-Gamma PAC especially in S1, suggesting the emergence of a non-physiological coupling which is counter intuitively enhanced by the stimulation. Additional experiments involving awake behaving animals are necessary to better characterize this interaction.

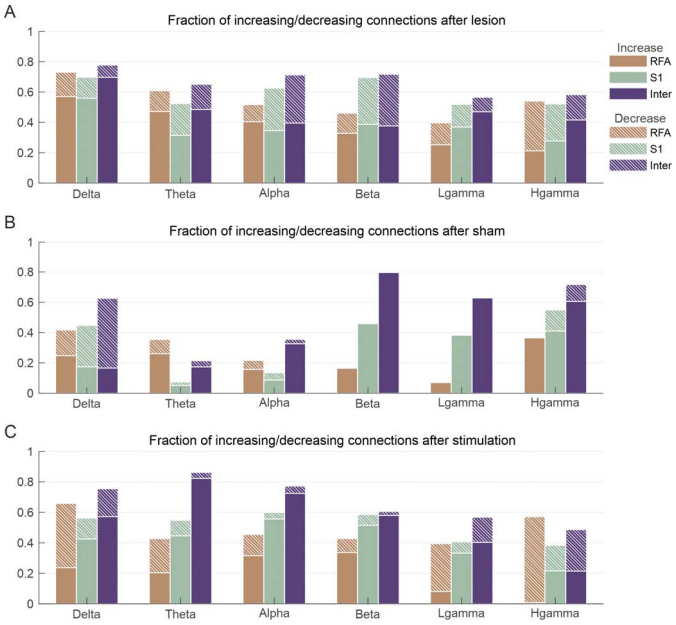

Fig. 7. Fraction of increasing/decreasing connections. Here the fraction of increasing and decreasing connections after the lesion, CTR and ADS are showed. Data is grouped by frequency bands and divided by location. The two values are stacked with the full bar representing increasing connections and the hatched bar the decreasing ones.

In the Control group we did not observe a clear response of PAC between the Basal2 and Basal1 periods. Interestingly, by computing the power envelope correlation, we observed a large increase in the inter- and intra-areas connectivity in the Delta band in the post-injury period, which shifted to that of Beta and Gamma bands between Basal2 and Basal1. The increases in Gamma activity, which is highly correlated with neural spiking, may be an indication of the overall increase in the excitatory response in regions within the peri-infarct area. Taken together, it is clear that there is a complex shift in activity that begins immediately after the injury and evolves over our recording session. Indeed, the observed increase in connectivity could be related to the communication loss induced by the lesion, which disrupts the structural connections between the two investigated cortical areas [46], [47].

ADS is thought to synchronize populations of neurons by directly coupling the intrinsic spiking activity in one region with the evoked spiking activity in a second region. To date, LFP signals have not been characterized following application of ADS. Here, the stimulation seems to stabilize or even reduce the overall signal power, which is somewhat surprising as the stimulation should be inducing even more activity than in the control conditions. Interestingly, ADS amplified the Theta-Gamma PAC both between and within our recorded areas. Additionally, we observed an increase in the synchronization observed in the Delta, Theta and Alpha bands, roughly corresponding to the range of stimulation frequencies observed during the stimulation period, suggesting that this one hour period had a carry-over effect on the intra-areal synchronization. Coupled with the lack of synchronous Gamma, increases measured by PEC after stimulation suggests that there may be a compensatory effect of the stimulation, normalizing the disturbance induced by the lesion.

While ADS has shown to be effective for facilitating long-term functional motor recovery, the present results suggest that this type of closed-loop stimulation may be effective as an immediate treatment for dysfunctional activity stemming from acquired brain injury. Further investigation is required to fully characterize the mechanistic properties of ADS for modulating activity in the acute periods after injury, especially in conditions not modulated by effects of the surgical anesthesia. Ultimately, understanding how stimulation may modulate brain network connectivity in normal and injured conditions will lead to novel treatments for many intractable neurological conditions.

ACKNOWLEDGMENT

The authors would like to thank Dr. Fellin and his group at IIT for hosting part of our experiments in his laboratory.

REFERENCES

[1] A. Averna *et al.*, "Entrainment of network activity by closed-loop microstimulation in healthy ambulatory rats," *Cerebral Cortex*, vol. 31, no. 11, pp. 5042–5055, Oct. 2021.
[2] *Neurological Disorders: Public Health Challenges*. World Health Org., Geneva, Switzerland, 2006.
[3] E. J. Benjamin *et al.*, "Heart disease and stroke statistics—2017 update: A report from the American heart association," *Circulation*, vol. 135, no. 10, pp. e146–e603, 2017.
[4] E. Bullmore and O. Sporns, "Complex brain networks: Graph theoretical analysis of structural and functional systems," *Nature Rev. Neurosci.*, vol. 10, no. 3, pp. 186–198, Mar. 2009.
[5] M. Catani and D. H. Ffytche, "The rises and falls of disconnection syndromes," *Brain*, vol. 128, no. 10, pp. 2224–2239, Oct. 2005.
[6] S. C. Cramer and E. P. Bastings, "Mapping clinically relevant plasticity after stroke," *Neuropharmacology*, vol. 39, no. 5, pp. 842–851, Apr. 2000.
[7] R. S. Marshall, G. M. Perera, R. M. Lazar, J. W. Krakauer, R. C. Constantine, and R. L. DeLaPaz, "Evolution of cortical activation during recovery from corticospinal tract infarction," *Stroke*, vol. 31, no. 3, pp. 656–661, Mar. 2000.
[8] R. J. Nudo, "Recovery after brain injury: Mechanisms and principles," *Frontiers Hum. Neurosci.*, vol. 7, p. 887, Dec. 2013.
[9] J. Jolkkonen and G. Kwakkel, "Translational hurdles in stroke recovery studies," *Transl. Stroke Res.*, vol. 7, no. 4, pp. 331–342, Aug. 2016.
[10] D. L. Adkins-Muir and T. A. Jones, "Cortical electrical stimulation combined with rehabilitative training: Enhanced functional recovery and dendritic plasticity following focal cortical ischemia in rats," *Neurolog. Res.*, vol. 25, no. 8, pp. 780–788, Dec. 2003.
[11] F. C. Hummel and L. G. Cohen, "Non-invasive brain stimulation: A new strategy to improve neurorehabilitation after stroke?" *Lancet Neurol.*, vol. 5, no. 8, pp. 708–712, Aug. 2006.
[12] F. Hummel *et al.*, "Effects of non-invasive cortical stimulation on skilled motor function in chronic stroke," *Brain*, vol. 128, no. 3, pp. 490–499, Mar. 2005.
[13] D. J. Guggenmos *et al.*, "Restoration of function after brain damage using a neural prosthesis," *Proc. Nat. Acad. Sci. USA*, vol. 110, no. 52, pp. 21177–21182, 2013.
[14] G. Panuccio, M. Semprini, L. Natale, S. Buccelli, I. Colombi, and M. Chiappalone, "Progress in neuroengineering for brain repair: New challenges and open issues," *Brain Neurosci. Adv.*, vol. 2, May 2018, Art. no. 2398212818776475.
[15] A. Averna *et al.*, "Differential effects of open- and closed-loop intracortical microstimulation on firing patterns of neurons in distant cortical areas," *Cerebral Cortex*, vol. 30, no. 5, pp. 2879–2896, May 2020.
[16] G. Buzsáki and B. O. Watson, "Brain rhythms and neural syntax: Implications for efficient coding of cognitive content and neuropsychiatric disease," *Dialogues Clin. Neurosci.*, vol. 14, no. 4, p. 345, 2012.
[17] O. Jensen and L. L. Colgin, "Cross-frequency coupling between neuronal oscillations," *Trends Cognit. Sci.*, vol. 11, no. 7, pp. 267–269, Jul. 2007.
[18] J. Hipp, D. Hawellek, M. Corbetta, M. Siegel, and A. Engel, "Large-scale cortical correlation structure of spontaneous oscillatory activity," *Nature Neurosci.*, vol. 15, pp. 884–890, May 2012.

[19] C. Watson and G. Paxinos, *The Rat Brain in Stereotaxic Coordinates: Hard Cover Edition*. Amsterdam, The Netherlands: Elsevier, 2006.
[20] G. Gilmour, S. Iversen, M. Oneill, M. Oneill, M. Ward, and D. Bannerman, "Amphetamine promotes task-dependent recovery following focal cortical ischaemic lesions in the rat," *Behavioural Brain Res.*, vol. 165, no. 1, pp. 98–109, Nov. 2005.
[21] P.-C. Fang, S. Barbay, E. J. Plautz, E. Hoover, S. M. Strittmatter, and R. J. Nudo, "Combination of NEP 1–40 treatment and motor training enhances behavioral recovery after a focal cortical infarct in rats," *Stroke*, vol. 41, no. 3, pp. 544–549, Mar. 2010.
[22] V. Shirhatti, A. Borthakur, and S. Ray, "Effect of reference scheme on power and phase of the local field potential," *Neural Comput.*, vol. 28, no. 5, pp. 882–913, May 2016.
[23] F. Tadel, S. Baillet, J. C. Mosher, D. Pantazis, and R. M. Leahy, "Brainstorm: A user-friendly application for MEG/EEG analysis," *Comput. Intell. Neurosci.*, vol. 2011, pp. 1–13, Oct. 2011.
[24] G. Foffani, "300-Hz subthalamic oscillations in Parkinson's disease," *Brain*, vol. 126, no. 10, pp. 2153–2163, Jun. 2003.
[25] A. C. E. Onslow, R. Bogacz, and M. W. Jones, "Quantifying phase-amplitude coupling in neuronal network oscillations," *Prog. Biophys. Mol. Biol.*, vol. 105, nos. 1–2, pp. 49–57, Mar. 2011.
[26] R. T. Canolty *et al.*, "High gamma power is phase-locked to theta oscillations in human neocortex," *Science*, vol. 313, no. 5793, pp. 1626–1628, Sep. 2006.
[27] I. Colombi, F. Tinarelli, V. Pasquale, V. Tucci, and M. Chiappalone, "A simplified *in vitro* experimental model encompasses the essential features of sleep," *Frontiers Neurosci.*, vol. 10, p. 315, Jul. 2016.
[28] I. Colombi, T. Nieus, M. Massimini, and M. Chiappalone, "Spontaneous and perturbational complexity in cortical cultures," *Brain Sci.*, vol. 11, no. 11, p. 1453, Nov. 2021.
[29] M. Chiappalone, P. Massobrio, and S. Martinoia, "Network plasticity in cortical assemblies," *Eur. J. Neurosci.*, vol. 28, no. 1, pp. 221–237, Jul. 2008.
[30] Z. Yu, M. Guindani, S. F. Grieco, L. Chen, T. C. Holmes, and X. Xu, "Beyond t test and ANOVA: Applications of mixed-effects models for more rigorous statistical analysis in neuroscience research," *Neuron*, vol. 110, no. 1, pp. 21–35, Jan. 2022.
[31] M. Krzywinski, N. Altman, and P. Blainey, "Nested designs," *Nature Methods*, vol. 11, no. 10, pp. 977–979, 2014.
[32] E. Aarts, M. Verhage, J. V. Veenvliet, C. V. Dolan, and S. van der Sluis, "A solution to dependency: Using multilevel analysis to accommodate nested data," *Nature Neurosci.*, vol. 17, no. 4, pp. 491–496, Apr. 2014.
[33] S. T. Carmichael and M.-F. Chesselet, "Synchronous neuronal activity is a signal for axonal sprouting after cortical lesions in the adult," *J. Neurosci.*, vol. 22, no. 14, pp. 6062–6070, Jul. 2002.
[34] D. S. Ramanathan *et al.*, "Low-frequency cortical activity is a neuromodulatory target that tracks recovery after stroke," *Nature Med.*, vol. 24, no. 8, pp. 1257–1267, Aug. 2018.
[35] P. Khanna, D. Totten, L. Novik, J. Roberts, R. J. Morecraft, and K. Ganguly, "Low-frequency stimulation enhances ensemble co-firing and dexterity after stroke," *Cell*, vol. 184, no. 4, pp. 912–930, 2021.
[36] M. Bönstrup *et al.*, "Low-frequency brain oscillations track motor recovery in human stroke," *Ann. Neurol.*, vol. 86, no. 6, pp. 853–865, Dec. 2019.
[37] N. Axmacher *et al.*, "Cross-frequency coupling supports multi-item working memory in the human hippocampus," *Proc. Nat. Acad. Sci. USA*, vol. 107, no. 7, pp. 3228–3233, Feb. 2010.
[38] R. T. Canolty and R. T. Knight, "The functional role of cross-frequency coupling," *Trends Cognit. Sci.*, vol. 14, no. 11, pp. 506–515, Nov. 2010.
[39] J. E. Lisman and O. Jensen, "The theta-gamma neural code," *Neuron*, vol. 77, no. 6, pp. 1002–1016, Mar. 2013.
[40] A. B. L. Tort, R. W. Komorowski, J. R. Manns, N. J. Kopell, and H. Eichenbaum, "Theta–gamma coupling increases during the learning of item–context associations," *Proc. Nat. Acad. Sci. USA*, vol. 106, no. 49, pp. 20942–20947, Dec. 2009.
[41] T. E. Özkurt *et al.*, "High frequency oscillations in the subthalamic nucleus: A neurophysiological marker of the motor state in Parkinson's disease," *Exp. Neurol.*, vol. 229, pp. 324–331, Jun. 2011.
[42] A. I. Yang, N. Vanegas, C. Lungu, and K. A. Zaghloul, "Beta-coupled high-frequency activity and beta-locked neuronal spiking in the subthalamic nucleus of Parkinson's disease," *J. Neurosci.*, vol. 34, no. 38, pp. 12816–12827, Sep. 2014.
[43] J. López-Azcárate *et al.*, "Coupling between beta and high-frequency activity in the human subthalamic nucleus may be a pathophysiological mechanism in Parkinson's disease," *J. Neurosci.*, vol. 30, pp. 6667–6677, May 2010.
[44] B. C. M. van Wijk *et al.*, "Subthalamic nucleus phase–amplitude coupling correlates with motor impairment in Parkinson's disease," *Clin. Neurophysiol.*, vol. 127, no. 4, pp. 2010–2019, Apr. 2016.
[45] A. Averna *et al.*, "Influence of inter-electrode distance on subthalamic nucleus local field potential recordings in Parkinson's disease," *Clin. Neurophysiol.*, vol. 133, pp. 29–38, Jan. 2022.
[46] J. C. Griffis, N. V. Metcalf, M. Corbetta, and G. L. Shulman, "Structural disconnections explain brain network dysfunction after stroke," *Cell Rep.*, vol. 28, no. 10, pp. 2527–2540, 2019.
[47] J. C. Griffis, N. V. Metcalf, M. Corbetta, and G. L. Shulman, "Damage to the shortest structural paths between brain regions is associated with disruptions of resting-state functional connectivity after stroke," *NeuroImage*, vol. 210, Apr. 2020, Art. no. 116589.